

Turbulent Character of Wind Energy

Patrick Milan, Matthias Wächter, and Joachim Peinke

ForWind—Center for Wind Energy Research, Institute of Physics, University of Oldenburg, 26129 Oldenburg, Germany

(Received 15 August 2012; revised manuscript received 25 January 2013; published 26 March 2013)

Wind turbines generate electricity from turbulent wind. Large fluctuations, and, more importantly, frequent wind gusts cause a highly fluctuating electrical power feed into the grid. Such effects are the hallmark of high-frequency turbulence. Here we show evidence that it is the complex structure of turbulence that dominates the power output for one single wind turbine as well as for an entire wind farm. We illustrate the highly intermittent, peaked nature of wind power fed into the grid. Multifractal scaling is observed, as described initially by Kolmogorov's 1962 theory of turbulence. In parallel, we propose a stochastic model that converts wind speed signals into power output signals with appropriate multifractal statistics. As more and more wind turbines become integrated into our electric grids, a proper understanding of this intermittent power source must be worked out to ensure grid stability in future networks. Thus, our results stress the need for a profound understanding of the physics of turbulence and its impact on wind energy.

DOI: 10.1103/PhysRevLett.110.138701

PACS numbers: 88.50.Mp, 47.27.Jv, 88.50.gj, 92.60.hk

Introduction.—The environment is a central concern of our society. This is particularly true in the energy sector, as the consumption of fossil fuels continually increases. Of the alternatives being implemented, one of the serious candidates is wind energy. Wind energy is expanding rapidly worldwide and promises a sustained growth within the next decade [1]. Industrial efforts contribute to wind turbines being progressively upscaled into large, efficient power plants that feed large cities with renewable energy at an ever decreasing cost. As such, wind energy promises a contribution to the present and coming energetic challenges.

Our growing dependence on wind energy brings technical challenges that could not yet be tested on large scales. Current grids are mainly powered by few large generators whose input is controllable, i.e., hydraulic, gas, pit coal, and to some extent nuclear power plants. The energy stored in rotor inertia ensures grid stability in the range of seconds by the use of synchronous generators, balancing power generation and consumption automatically by frequency changes in the range of mHz. However, wind turbines operate within complex, uncontrollable wind fields. Most modern designs involve variable rotational speed in order to optimize aerodynamic performance and reduce mechanical loads. ac-dc-ac inverters must then be used between the generator and the grid to match the specified grid frequency, thus decoupling the rotating mechanical parts of wind turbines from the grid [2]. In this decoupled configuration, the controller of the wind turbine commonly operates freely to maximize power output; i.e., to follow the wind power fluctuations mostly regardless of the grid load. When a large amount of the traditional synchronous generators are replaced by decoupled wind turbine generators, the grid reactivity will be altered, thus making the generation and load balance difficult. To our knowledge, this is a new challenging problem for power grids that has not yet been

addressed. Furthermore, the typical reaction time of wind turbines is in seconds, so that the grid dynamics in this time range become more complex. Smart grid concepts should be designed to cope with large amounts of fluctuating, turbulentlike wind power. The first attempts can be found in, e.g., Refs. [3,4]. A virtual synchronous generator concept is proposed in Ref. [5]. Synchronization effects are addressed in Ref. [6]. Nevertheless, the complex nature of turbulent wind conditions, including extreme events have not been taken into account yet. In this Letter we point out that for the most efficient grid integration of wind energy, the physics of wind power fluctuations must be understood in detail.

More fundamentally, understanding and reliably predicting wind dynamics remains a central problem in order to forecast wind power. The widely used hypothesis of a spectral gap [7] allows us to conveniently separate the dynamics of microscale turbulence from mesoscale climatology. This hypothesis supports the historical use of ten-minute-averaged data records that supposedly contain all mesoscale dynamics without high-frequency turbulence. While mesoscale predictions are a central focus of energy meteorology, high-frequency fluctuations are seldom addressed. Wind energy standards like the International Electrotechnical Commission (IEC) norm [8] consider turbulent fluctuations as a random Gaussian field, far from what is observed on measurement data. In contrast to such standards, recent works like, e.g., Ref. [9] show that the statistics of atmospheric turbulence are at least as complex as those of homogeneous isotropic turbulence. The log-normal cascade model presented in Ref. [10] was successfully extended to atmospheric turbulence in Ref. [11]. References [12,13] suggest a multifractal cascade process in the atmosphere. Results in Ref. [14] support the idea of a universal cascade in the atmosphere, that could be modeled in Ref. [15]. This confirms the importance of turbulence

TABLE I. Data description for the data sets used with corresponding rated power P_r . The exact value of the rated powers P_r of the wind farm and turbine 1 could not be published following an agreement with the farm manager. The number of data points collected is provided as well as the duration and sampling frequency of the measurement campaign. The name of the wind speed and power output time series is given for further notice. The wind farm consists of 12 wind turbines spread over a rectangular area of about 4 km^2 , surrounded by rural flat terrain.

Data set	Rated power P_r	No. of data	Duration	Frequency	Wind speed	Power output
Wind farm	$\sim 25 \text{ MW}$	15.3×10^6	$\sim 8 \text{ months}$	1 Hz	...	P_{farm}
Turbine 1	$\sim 2 \text{ MW}$	15.2×10^6	$\sim 8 \text{ months}$	1 Hz	u	P
Turbine 2	2 MW	2.16×10^6	1 day	25 Hz	u_2	P_2

research for atmospheric wind. We will show how this affects wind power conversion.

We focus here on the aforementioned problem of fluctuations in time scales of seconds in atmospheric turbulence and how they transfer to the electric grid. After a brief description of wind turbine dynamics, a statistical analysis is presented. Our results are derived from data measured on operating wind turbines. The data sets used are presented in Table I [16].

Nonlinear wind turbine dynamics.—Modern wind turbines are designed to extract maximal power from the wind. The power contained in a volume of air of density ρ flowing at speed u through an area A is $P_{\text{wind}} = \frac{\rho}{2} A u^3$. The power coefficient c_p defines the ratio of power extracted $P = c_p P_{\text{wind}}$, for our data $c_p \approx 0.4$ [17]. It should be noted that current wind turbine designs focus on power extraction, so as to maximize the power output regardless of the load of the electric grid.

The conversion process $u \rightarrow P$ is commonly simplified to an average power curve $P(u)$. The IEC norm [19] defines such a power curve from 10 min averaged u and P signals, where faster fluctuations are already averaged out. References [20,21] observe that 2nd- and 3rd-order terms should be considered as well when averaging over a nonlinear power curve. Turbulent fluctuations imply a highly dynamical conversion process $u \rightarrow P$, making the cubiclike power curve oversimplified at high frequencies. Exemplary high-frequency signals are displayed in Fig. 1(a). It appears that the wind turbine converts wind fluctuations into power fluctuations. Apparently, the conversion dynamics take place at short time scales of seconds; see also the spectral analysis in Fig. 1(b). Wind speed and power output have a similar spectral (and correlation) behavior at low frequencies $f < 0.1 \text{ Hz}$, following the theoretical $-5/3$ law of turbulence from Kolmogorov 1941; i.e., $S(f) \sim f^{-5/3}$ [22].

The $-5/3$ spectrum of wind speed u_2 seems at first consistent with turbulence theory, although some care should be taken. The measurement was conducted close to the ground in the atmospheric boundary layer, where wall-bounded turbulence offers a more realistic description than homogeneous isotropic turbulence. However, Ref. [23] observes that for a wall-bounded flow with Reynolds number $Re = 10^6$, a fully-developed $-5/3$ spectrum is observed at large wave numbers $k > 0.5/z$, where z is the distance from the boundary. This is consistent with

results in Fig. 1(b) for u_2 ($Re \sim 10^7$), where a $-5/3$ spectrum is measured in the inertial subrange $f > 0.05 \text{ Hz}$. A flattening of the spectrum is observed for lower frequencies $f < 0.05 \text{ Hz}$, as observed also by Ref. [9]. As this is not of interest for our work here, we do not discuss further details on the effect of the boundary.

The spectrum of power output P_2 follows a power law behavior $S(f) \sim f^{-5/3}$ for low frequencies $f < 0.1 \text{ Hz}$, stressing the straightforward dynamics of the conversion process $P \propto u^3$ at such slow time scales [24]. However, the spectrum of P deviates from a power law behavior for higher frequencies $f > 0.1 \text{ Hz}$ where the dynamics of the turbine machinery come into play. Simply put, the reaction time of the 2 MW turbine (number 2) studied here is on the order of 10 s. This reaction time depends on the turbine design, size, etc., but was systematically found to be less than a minute for different multi-MW turbines. The fast reaction [25] is desired to maximize power production (instead of, e.g., power stability or mechanical load reduction, see Ref. [28]). As a result, fast wind fluctuations within the reaction time are partly filtered, and slower wind fluctuations are adiabatically converted into power output fluctuations. Thus the simple IEC power curve description can be used only at large time scales, whereas a physical model is necessary to model fast dynamics that

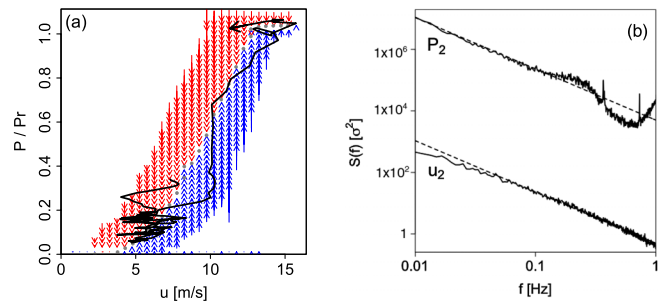


FIG. 1 (color online). (a) Three-minute trajectory of power output vs wind speed signals $P(t)$ and $u(t)$ for turbine 1. The drift field $D^{(1)}(P|u)$ calculated from Eq. (2) is represented in the background [blue (red) arrows for positive (negative) drift values]. Power values are normalized by the rated power P_r . See Supplemental Material at Ref. [46] for a movie of the conversion dynamics; (b) power spectra of wind speed u_2 (lower) and power output P_2 (upper) in log-log scale for turbine 2. $-5/3$ spectra are represented by dashed lines.

are largely dominated by the rotor inertia and the dynamics of the control system.

Modeling the conversion process $u \rightarrow P$ implies describing the turbine dynamics at the time scales where the turbine reacts. References [29,30] observe that it can be described simply as a response model; the power curve is seen as an attractor, around which the system fluctuates. We developed a stochastic model where the conversion process is simplified as a Langevin process for the power conditioned to fixed wind speeds

$$\frac{dP}{dt} = D^{(1)}(P|u) + \sqrt{D^{(2)}(P|u)}\Gamma, \quad (1)$$

where the Kramers-Moyal coefficients $D^{(n)}$ can be estimated without assumption from measurement data

$$D^{(n)}(P|u) = \lim_{\tau \rightarrow 0} \frac{1}{n!} \langle [P(t + \tau) - P(t)]^n | P(t) = P; u(t) = u \rangle. \quad (2)$$

Γ is taken as a Gaussian uncorrelated noise with mean value $\langle \Gamma(t) \rangle = 0$ and variance $\langle \Gamma(t)^2 \rangle = 2$; see Ref. [31]. The conversion process $u(t) \rightarrow P(t)$ is split into a deterministic drift $D^{(1)}$ plus some random fluctuations $\sqrt{D^{(2)}}\Gamma$. Figure 1(a) shows how turbine 1 converts wind speed into power output in a stochastic way. The drift matrix $D^{(1)}(P|u)$ models the conversion process with attractive fixed points [gray dots between blue (red) arrows for positive (negative) drift values]. The stochastic character of the conversion process is modeled through the diffusion matrix $D^{(2)}$. We present some results of the stochastic model in Figs. 2(c) and 2(d).

Feeding turbulence to the grid.—Turbulent flows are known to be intermittent, especially over short time scales. This can be observed on wind speed time series, which repeatedly transit between steady states and rapid gusts. Such gusty, intermittent behavior can be quantified through increments statistics. Wind speed increments

$u_\tau(t) = u(t + \tau) - u(t)$ quantify the change in wind speed u over a time scale τ . Extreme values of increments are seen as gusts. Increment PDFs (probability density functions) $f(u_\tau)$ quantify the probability of observing a given increment u_τ . We use normalized increments u_τ/σ_τ , where σ_τ is the standard deviation of u_τ , so that normalized increment PDFs can be compared to a normal distribution of standard deviation 1. We define in a similar fashion increments of power output over a time scale τ as $P_\tau(t) = P(t + \tau) - P(t)$ and their corresponding increment PDFs $f(P_\tau)$.

Excerpts of increment time series are presented in Figs. 2(a) and 2(b) for $\tau = 8$ sec. Power increments look more intermittent than wind speed increments, exhibiting a clearer alternation between steady and gusty phases. Increment PDFs in Fig. 2(c) depart largely from the normal distribution, as they possess exponential-like *heavy tails*. These tails reach extreme values, corresponding to a higher-than-normal probability to record an extreme event. While wind speed increments look moderately intermittent, power increments are highly intermittent. Extreme events up to about $10\sigma_\tau$ are recorded in the wind speed signal u , and up to about, respectively, $20\sigma_\tau$ and $15\sigma_\tau$ for P and P_{farm} . While such extreme values cannot be observed in normal-distributed processes over reasonably long times, they are measured regularly in wind power signals. These extreme, intermittent statistics are reproduced mostly well by the stochastic model of power output in Eq. (1). The stochastic model was presented for a single wind turbine in Ref. [32]. Results for wind farm modeling are equally satisfactory as for a single wind turbine, making the model a promising tool for grid integration. Further details for the wind farm model will be published in Ref. [33].

An overview of the most extreme increment values measured is presented in Table II. Within the measurement period, the wind speed changed by about 11 m/s within 8 sec. In reaction to such a wind gust, the wind turbine can change its power production by about 80%, and the wind

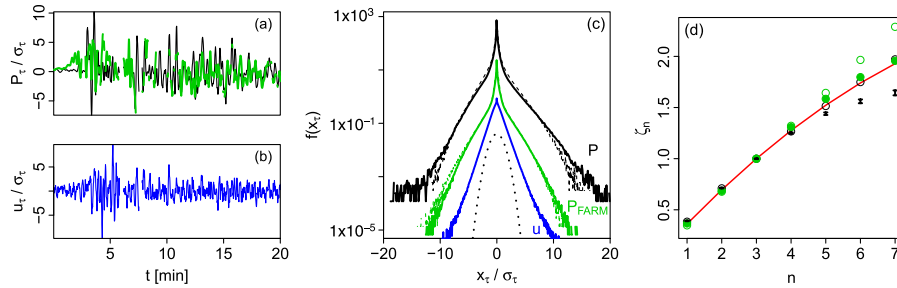


FIG. 2 (color online). Excerpts of normalized increment time series for $\tau = 8$ sec (a) of power output P (black line) and P_{farm} (bold green line), (b) of wind speed u (blue line), (c) increment PDFs for P (upper black), P_{farm} (middle green), and u (lower blue) in lin-log scale. The results of the stochastic model in Eq. (1) are displayed for P and P_{farm} by the thin dashed curves. The PDFs are arbitrarily shifted upwards for clarity. A normal distribution is displayed by the lower black dots; (d) scaling exponents ζ_n for P measured (black error bars) and modeled (open black dots), and P_{farm} measured (full green dots) and modeled (open green dots). The dot size is chosen on the order of the statistical error. Kolmogorov's 1962 model is represented (red line). $S_n(\tau)$ were estimated for $\tau \in \{1; 120\}$ s, where Eq. (3) is satisfied. $\zeta_3 = 1$ following the ESS convention. In the extended self-similarity convention, possible deviations from exact self-similarity are circumvented by studying only the relation of the structure functions to their third order counterpart. Information can thus be gained on the multifractality of a process even if self-similarity is not strictly achieved.

TABLE II. Absolute value of the most extreme increments measured over a time scale τ during the measurement period of 8 months. The power increments are given in percent of the corresponding rated power for the turbine and the farm. Occasional overshoots slightly above rated power justify power increments larger than 100%.

Most extreme increment	$\tau = 1$ s	$\tau = 8$ s	$\tau = 32$ s	$\tau = 128$ s
Wind speed u_τ (m/s)	3.5	11.1	11.4	14.7
Turbine power P_τ (%)	24.8	82.5	106.6	108.8
Farm power $P_{\text{farm},\tau}$ (%)	8	22.8	33	55.3

farm by about 23%. The wind farm can change its power output by about 50% within 2 min.

Statistically speaking, the intermittency of a turbulent process can be related to the scaling of its structure functions [34]

$$S_n(\tau) = \langle |P_\tau|^n \rangle \sim S_3(\tau)^{\zeta_n} \quad (3)$$

over the inertial range of a turbulent cascade. Multifractality is related to the scaling exponents ζ_n being a nonlinear [36] function of n [22]. Scaling exponents are displayed in Fig. 2(d) for P and P_{farm} . A rather good agreement with Kolmogorov's 1962 model is observed for the power output signals suggesting that the wind power is a turbulent multifractal process. In the case of the wind farm, the measured output is multifractal, yet the modeled signal is almost monofractal. Our current stochastic model tends to reproduce a bit less multifractality than the measurement [38]. The nonlinear, multifractal scaling measured emerges from mixing turbulent, atmospheric dynamics additionally with a nonlinear power conversion $u \rightarrow P$. Wind turbines convert multifractal turbulent wind into multifractal, turbulentlike power.

Besides the multifractal scaling also the absolute values of the flatness (or kurtosis) of the increment PDF $F(\tau) = \frac{S_4(\tau)}{S_2(\tau)^2}$ is a crucial parameter. $F(\tau) = 3$ for the normal distribution, and increases for more heavy-tailed PDFs. The flatness of increment PDFs is then a direct measure of intermittency. Flatness values beyond, respectively, 40 and 20 are observed for wind turbine and wind farm outputs for time scales of a few seconds. The flatness does not extend beyond 10 for atmospheric wind speeds, stressing the higher intermittency of power outputs compared to turbulent wind. As such, wind turbines do not only transfer wind intermittency to the grid, but also increase it. This point cannot be seen in the scaling analysis. The increased intermittency is attributed to the nonlinear conversion process and the fast reaction time. Wind power intermittency was observed in Ref. [39] for the output of a single wind turbine but to a lesser extent due to the limited amount of data of only 2 days. However, intermittency in wind farm output was to our knowledge not yet observed. Wind farm intermittency is somewhat counterintuitive, as one expects that the act of summing up distant turbines would randomize their cumulative output. This is not observed,

arguably due to the long-range correlations observed in atmospheric winds. The wind farm covers an area of about 4 km², meaning that the 12 neighboring turbines are driven by similar winds, and they produce power outputs that are strongly correlated. We speculate that cumulative wind power should remain intermittent on spatial scales as large as the correlation length of atmospheric wind. (References [40,41] observe that such correlations are on the order of 600 km.) Reference [42] also observes power intermittency on a 300-km large wind cluster of 1000 MW at a time scale $\tau = 15$ min, showing that intermittency persists at large spatial and temporal scales. This has a large impact on stability in largely wind-powered grids.

Conclusion.—Wind turbines convert a turbulent wind speed u into a turbulentlike electrical power P . For time scales larger than several minutes, i.e., larger than the regulating time of the control system, power dynamics can be considered to follow adiabatically the wind dynamics with similar $-5/3$ spectral properties; therefore, the necessary information is given by the standard average power curve $P(u)$. For the smaller time scales, where the control system of the wind conversion systems interacts dynamically with wind fluctuations, we find that the power output has highly intermittent increment PDFs with multifractal scaling close to Kolmogorov's log-normal laws. We promote a stochastic model for these power dynamics as a promising tool for wind energy integration and grid planning. Although the statistical features of the power data are qualitatively similar to the wind field itself, the magnitude of extreme events and of kurtosis are up to four times higher, showing that wind turbines transfer intermittency to the grid and amplify it.

The intermittent properties of wind power are maintained on the scale of an entire wind farm. We observed that the power output of the wind farm changed by 50% in only 2 min once over several months. These results go against the deceptive argument that clustering wind turbines averages out their turbulent fluctuations. The strong correlations between neighboring turbines violate the central limit theorem, and the cumulative farm power is largely non-Gaussian. Extreme power changes up to 15 standard deviations are observed within seconds with a kurtosis value of 20. There are indications that such effects persist up to much larger spatiotemporal scales, on the order of the correlation length of the atmosphere of hundreds of kilometers.

These aspects remain overseen in the wind energy community. From the physical point of view of complex systems this situation is reminiscent of the situation in economics some years ago. There it has also been important to realize the intermittent and multifractal nature of the stock market [43–45]. As for the stock market and the economical system, the higher-than-normal occurrence of wind power gusts needs to be accounted for in order to maintain power stability in future grids. Adapted solutions such as smart curtailment or energy storage remain to be developed with a focus on power stability. Such solutions must be properly dimensioned to match the extreme fluctuations observed. Otherwise, electrical intermittency and

grid instability will grow larger with the ongoing exploitation of the wind resource.

We thank the Land of Lower Saxony, the German Ministry for Environment, and the German Ministry for Education and Research for funding this research project. We also thank Deutsche Windtechnik AG Bremen for providing us with wind turbine data. This work relies greatly on the pioneering work of Edgar Anahua, Stephan Barth, and Julia Gottschall in wind energy applications. We would also like to thank Allan Morales, Tanja Mücke, Michael Hölling, Björn Witha, Bernd Orlik, and Mohammad Reza Rahimi Tabar for the many fruitful discussions.

- [1] W. W. E. Association, "World Wind Energy Report 2010," 2011.
- [2] E. Hau, *Wind Turbines: Fundamentals, Technologies, Application, Economics* (Springer, New York, 2006), 2nd ed.
- [3] J. Liu, B. H. Krogh, and B. E. Ydstie, *American Control Conference, San Francisco, CA*, 2011.
- [4] A. M. Giacomo, S. M. Amin, and B. F. Wollenberg, *American Control Conference, San Francisco, CA*, 2011.
- [5] K. Sakimoto, Y. Miura, and T. Ise, *8th International Conference on Power Electronics-ECCE Asia, Jeju, South Korea*, 2011.
- [6] M. Rohden, A. Sorge, M. Timme, and D. Witthaut, *Phys. Rev. Lett.* **109**, 064101 (2012).
- [7] I. Van der Hoven, *J. Meteorol.* **14**, 160 (1957).
- [8] IEC 61400-1, Wind turbines. Part 1: Design requirements, International Electrotechnical Commission, 2005, 3rd ed.
- [9] A. Morales, M. Wächter, and J. Peinke, *Wind Energy* **15**, 391 (2012).
- [10] B. Castaing, Y. Gagne, and E. J. Hopfinger, *J. Phys. D* **46**, 177 (1990).
- [11] F. Böttcher, St. Barth, and J. Peinke, *Stoch. Environ. Res. Ris. Assess.* **21**, 299 (2007).
- [12] S. Lovejoy, D. Schertzer, and J. D. Stanway, *Phys. Rev. Lett.* **86**, 5200 (2001).
- [13] S. Lovejoy, D. Schertzer, V. Allaire, T. Bourgeois, S. King, J. Pinel, and J. Stolle, *Geophys. Res. Lett.* **36**, L01801 (2009).
- [14] J.-F. Muzy, R. Baïle, and P. Poggi, *Phys. Rev. E* **81**, 056308 (2010).
- [15] R. Baïle, J. F. Muzy, and P. Poggi, *Wind Energy* **14**, 719 (2011).
- [16] It should be noted that some data samples have not been recorded during the measurement campaign for turbine 1 and the wind farm. All the algorithms used here are robust against such limitations.
- [17] The physical limit for the efficiency of a wind turbine is known as the Betz limit $c_p \leq 0.59$ [18].
- [18] T. Burton, D. Sharpe, N. Jenkins, and E. Bossanyi, *Wind Energy Handbook* (Wiley, New York, 2001).
- [19] IEC 61400-12, Wind Turbines—Part 12: Power Performance Measurements of Electricity Producing Wind Turbines. International Electrotechnical Commission, 2005.
- [20] A. Rosen and Y. Sheinman, *J. Wind Eng. Ind. Aerodyn.* **51**, 287 (1994).
- [21] F. Böttcher, J. Peinke, D. Kleinhans, and R. Friedrich, in *Wind Energy*, edited by J. Peinke, P. Schaumann, and

- St. Barth Proceedings of the Euromech Colloquium (Springer, Berlin, 2007), pp. 179–182.
- [22] U. Frisch, *Turbulence: The Legacy of A. N. Kolmogorov* (Cambridge University Press, Cambridge, England, 1995).
- [23] I. Marusic, B. J. McKeon, P. A. Monkewitz, H. M. Nagib, A. J. Smits, and K. R. Sreenivasan, *Phys. Fluids* **22**, 065103 (2010).
- [24] It can be seen numerically that for a self-similar signal $x(t)$ with power spectral density $S(f) \propto f^{-\beta}$, the spectral behavior of $\alpha[x(t)]^3$ remains $S(f) \sim f^{-\beta}$.
- [25] Their seemingly constant rotational speed misleads one into thinking that wind turbines work at a steady regime. In reality, fast wind speed fluctuations generate fast mechanical torque fluctuations on the rotor, which are then converted into fast power fluctuations by the generator; see Refs. [26,27] for a statistical analysis of torque dynamics.
- [26] T. Mücke, D. Kleinhans, and J. Peinke, *Wind Energy* **14**, 301 (2011).
- [27] M. Wächter, H. Heißelmann, M. Hölling, A. Morales, P. Milan, T. Mücke, J. Peinke, N. Reinke, and P. Rinn, *J. Turbul.* **13**, N26 (2012).
- [28] F. Bianchi, H. De Battista, and R. Mantz, *Wind Turbine Control Systems* (Springer, Berlin, 2006), 2nd ed.
- [29] E. Anahua, S. Barth, and J. Peinke, *Wind energy* **11**, 219 (2008).
- [30] J. Gottschall and J. Peinke, *Environ. Res. Lett.* **3**, 015005 (2008).
- [31] R. Friedrich, J. Peinke, M. Sahimi, and M. R. R. Tabar, *Phys. Rep.* **506**, 87 (2011).
- [32] P. Milan, M. Wächter, and J. Peinke, Proceedings of EWEA, Brussels, 2011.
- [33] P. Milan, M. Wächter, and J. Peinke (to be published).
- [34] Various conventions exist for the structure functions $S_n(\tau)$ and their corresponding scaling exponents ζ_n . We choose the *extended self-similarity* convention here [35].
- [35] R. Benzi, S. Ciliberto, R. Tripiccione, C. Baudet, F. Massaioli, and S. Succi, *Phys. Rev. E* **48**, R29 (1993).
- [36] Linear scaling exponents $\zeta_n = n/3$ are first proposed in Kolmogorov's monofractal model of 1941. Kolmogorov's multifractal model of 1962 then includes a nonlinear relation $\zeta_n = \frac{n}{3} - \frac{\mu}{18}n(n-3)$, where the nonlinear correction directly controls intermittency through the intermittency factor $\mu = 2 - \zeta_6 \approx 0.26$ [37].
- [37] A. Arneodo *et al.*, *Europhys. Lett.* **34**, 411 (1996).
- [38] If necessary, the noise term $\Gamma(t)$ in the Langevin equation (1) can be modified to a non-Gaussian, correlated, or multifractal noise in order to recover the multifractality.
- [39] J. Gottschall and J. Peinke, *J. Phys. Conf. Ser.* **75**, 012045 (2007).
- [40] R. Baïle and J.-F. Muzy, *Phys. Rev. Lett.* **105**, 254501 (2010).
- [41] R. Kavasseri and R. Nagarajan, *IEEE Trans. Circuits Syst. I* **51**, 2255 (2004).
- [42] O. Kamps, Proceedings of the Euromech Colloquium (to be published).
- [43] R. N. Mantegna and H. E. Stanley, *Nature (London)* **376**, 46 (1995).
- [44] S. Ghashghaie, W. Breymann, J. Peinke, P. Talkner, and Y. Dodge, *Nature (London)* **381**, 767 (1996).
- [45] T. Lux and M. Marchesi, *Nature (London)* **397**, 498 (1999).
- [46] See Supplemental Material at <http://link.aps.org/supplemental/10.1103/PhysRevLett.110.138701> for a movie of the conversion dynamics.